Optoelectronics

DOI: 10.1002/ange.201304301

Conductance Switching and Mechanisms in Single-Molecule Junctions**

Chuancheng Jia, Jinying Wang, Changjiang Yao, Yang Cao, Yuwu Zhong, Zhirong Liu, Zhongfan Liu, and Xuefeng Guo**

From its very start, one of the most intriguing motivations of molecular electronics is to provide unique and low-cost solutions for electronic functions based on molecules, such as diodes, transistors, switches, and memristors, since molecules are probably the smallest units still capable of offering a rich structural variety.[1,2] However, the ability to control the conductance of molecules at the molecular level by an external mode is still a formidable challenge in this field. Here we report the observation of reproducible conductance switching triggered by external light on a new platform of graphene–molecule junctions, where three photochromic diarylethene derivatives with different substituents are used as key elements. Analyses of both transition voltage spectroscopy and first-principles calculations consistently reveal tunable molecule–electrode coupling, thus demonstrating the photogated inflection (V_{trans}) transition when the charge-transport mechanism changes from direct to Fowler–Nordheim (F-N) tunneling.

We chose diarylethene derivatives as photosensitive molecular bridges because they, as a typical family of photochromic molecules, can undergo reversible transitions between two distinct isomers with open/closed conformations when exposed to light irradiation (Figure 1a).[3] The closed isomer is nearly planar, but the open isomer adopts a bent conformation with its thiophene rings twisted about 61° out of the plane from the cyclopentene ring. Correspondingly, these two isomers display different absorption spectra, that of the closed form extends towards longer wavelengths up to the visible region, suggesting the delocalization of π electrons over the entire structure (see Figure S1 in the Supporting Information). In the open form, however, delocalization of the π electrons is restricted to each half of the molecule and electronic communication through the unsaturated bond of the middle ring is interrupted. Another remarkable feature of the diarylethene molecules used in this study is that only negligible changes in the molecular length (≤ 0.2 Å) happen when they switch back-and-forth between open/closed states (Figure S2 and Table S1). In conjunction with their superior thermal stability and fatigue resistance, these significant electronic and structural properties place diarylethene molecules as ideal candidates for building light-driven molecular switches as demonstrated theoretically[4] and experimentally.[5] However, a longstanding challenge is to conserve these promising properties in solution when the diarylethene molecules are sandwiched between solid-state molecular-scale electrodes.[2,6] One major reason is due to the quenching effect of the photoexcited states of the diarylethene molecules by the electrodes,[5e,f] which strongly stresses the importance of the molecule–electrode coupling strength to the device performance.[2,7]

To tailor the energy level alignments at the molecule–electrode interface, in this study we intend to modify diarylethene backbones with rationally designed side and anchoring groups (**1**–**3** in Figure 1b). This modification has two specific considerations. The first is to substitute the hydrogenated cyclopentene in **1** by the fluorinated unit (**2**). In comparison with the hydrogenated cyclopentene, the fluorinated unit is electron-withdrawing and thereby decreases the electron density on the central alkene unit and increases the fatigue resistance of the photochromic properties.[3a] The second is to further introduce a methylene group (CH_2) between the terminal amine group and the functional center on each side (**3**). The incorporation of the saturated CH_2 groups can cut off π-electron delocalization, thus largely decoupling the electronic interaction between molecules and electrodes. Theoretical calculations were performed to predict the electronic structures of the molecule–electrode contacts as shown in Figure 1c (Table S2). Indeed, the energy levels of **2** are lower than those of **1** because of the electron-withdrawing effect of the fluorinated unit, which is consistent with electrochemical measurements of similar systems.[8] For **3**, the energy levels are even lower. More importantly, the calculated molecular orbital diagrams reveal a lower orbital density of states (DOS) at the C sites of the CH_2 groups (Figure 1c), which implies that the CH_2 groups decrease the strong electronic coupling between diarylethene molecules and electrodes. These results demonstrate the potential of molecular engineering as an efficient tool for tuning the molecule–electrode coupling strength. This tuna-

[*] C. Jia,[+] J. Wang,[+] Y. Cao, Prof. Z.-R. Liu, Prof. Z.-F. Liu, Prof. X.-F. Guo
Center for NanoChemistry
Beijing National Laboratory for Molecular Sciences
State Key Laboratory for Structural Chemistry of Unstable and Stable Species, College of Chemistry and Molecular Engineering, Peking University
Beijing 100871 (P. R. China)
E-mail: zfliu@pku.edu.cn
guoxf@pku.edu.cn
C. Yao, Prof. Y.-W. Zhong
Institute of Chemistry, Chinese Academy of Sciences
Beijing 100190 (P. R. China)

[+] These authors contributed equally to this work.

[**] We acknowledge primary financial support from MOST (grant number 2012CB921404) and NSFC (grant numbers 21225311 and 51121091).

Supporting information for this article is available on the WWW under http://dx.doi.org/10.1002/anie.201304301.

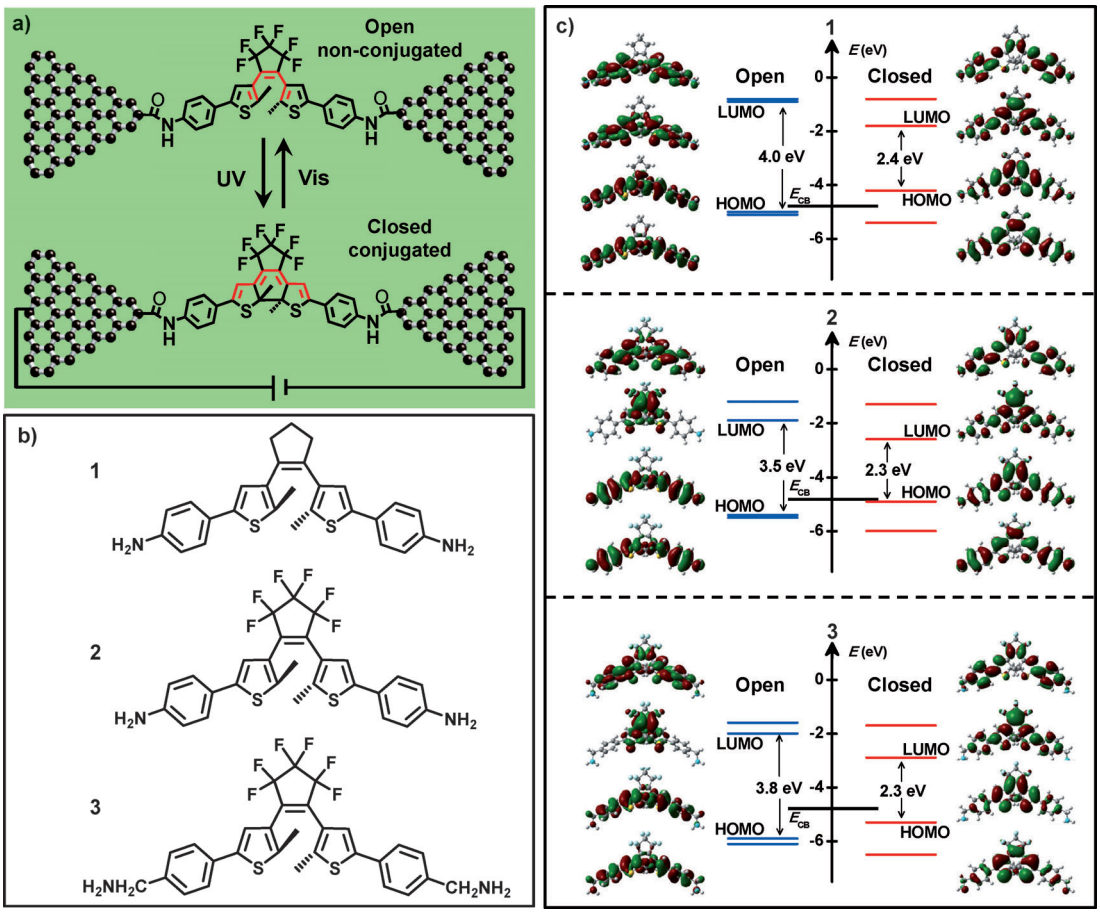

Figure 1. a) Switching of graphene–diarylethene junctions. b) Molecular structures of **1**–**3**. c) Calculated molecular energy levels and related molecular orbital diagrams (LUMO + 1, LUMO, HOMO and HOMO-1) of **1**–**3**. E_{CB} is the work function of graphene.

bility is of great importance in molecular junctions because it allows precise construction of the contact interface as well as adjustment of the interfacial electronic structure and exploration of the intrinsic transport mechanism, depending on the molecular structure to be used.

Syntheses of **1**–**3** with the requisite amine anchors are detailed in the Supporting Information. The graphene–diarylethene junctions were fabricated by a dash-line lithographic (DLL) method described in detail elsewhere,[9] using chemical vapor deposition (CVD) grown high-quality single-layer graphenes on copper foils.[10] One important feature of this approach is that the contacts made by covalent amide bond formation are robust and thus can tolerate broad external stimuli. In conjunction with the remarkable properties of graphene electrodes, the ease of device fabrication and the device stability position graphene–molecule junctions as a new-generation testbed for molecular electronics. On the basis of the statistical data, the average connection yields were found at 25 % for **1**, 25 % for **2,** and 31 % for **3**, which are reasonable to afford single-molecule junctions in most cases as detailed in the Supporting Information.[9]

Figure 2a shows the comparison of the current–voltage (*I*–*V*) curves of a **2**-reconnected molecular junction before and after irradiation of UV light from a low-intensity handheld UV lamp (about 100 μW cm^{-2}, 365 nm), respectively (More data for **1** or **3**-reconnected molecular junctions can be found in Figures S3–S5). Remarkably, photoinduced significant consistent changes from the low-conductance (off) state to the high-conductance (on) state were observed for all the working devices. This observation should be ascribed to the isomerization from the open, unconjugated conformation to the closed, conjugated conformation under UV illumination (Figure 1a). To better understand the switching phenomenon through diarylethene molecules, the energy dependence of the transmission spectra at zero bias voltage was calculated as shown in Figure 2c,d and Figure S6. Clearly, the calculated transmission spectra of open and closed conformations are distinctively different near the Fermi level. Since the HOMO and LUMO of diarylethene molecules with open conformations are localized frontier orbitals (Figure 1c), which are not good conductive channels for electrons passing through the junctions, there is not any significant transmission channel located at the energy range from −0.05 to 2.00 eV (Figure 2c). On the contrary, the HOMO and LUMO of diarylethene molecules with closed conformations are delocalized π-conjugated orbitals (Figure 1c), which provide good conductive channels, thus leading to two significant transmission peaks located at each side of the Fermi level (about −0.05 eV and 1.2 eV; Figure 2d). For molecular electronic devices, the nearest transmission peaks at each side of the Fermi level

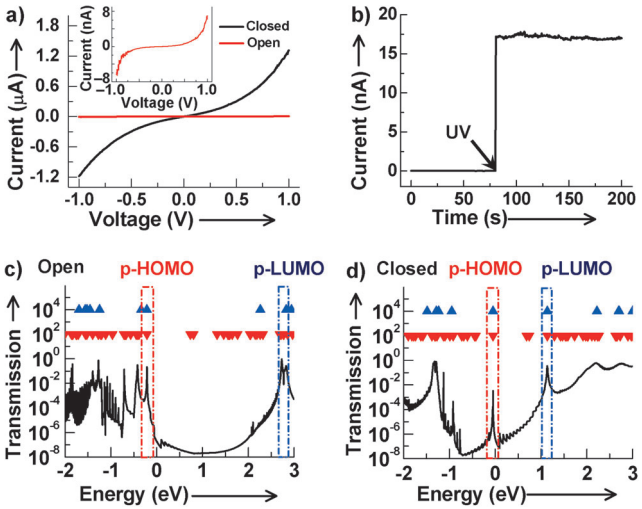

Figure 2. Switching properties of a **2**-reconnected molecular junction as a representative. a) *I–V* characteristics of **2** with open (red line) and closed (dark line) states at $V_G = 0$ V. The inset shows the enlarged *I–V* curve for the open state. b) The current-versus-time curve of the same device at $V_D = 50$ mV and $V_G = 0$ V. c–d) The zero-bias voltage transmission (T_0) spectra of **2**-reconnected junctions with c) open and d) closed configurations. Both open and closed isomers are constructed to have similar angles with graphene (Figure S7). The full red downward-pointing and full blue upward-pointing triangles stand for the energies of the MPSH and isolated molecules, respectively. The red and blue rectangles mark out the transmission peaks of p-HOMO and p-LUMO.

corresponds well to the HOMO and LUMO of the molecules. Then we further calculated the molecular projected self-consistent Hamiltonian (MPSH) spectra on the entire photochromic core between graphene electrodes (Figure S8). The perturbed HOMO (p-HOMO) and LUMO (p-LUMO) retain most features of the molecular orbitals, especially for p-HOMO. Because p-HOMOs are much closer to the Fermi level in all systems, they mainly dominate the carrier transport behavior at low bias voltages. On the basis of the theoretical results, consequently, it is no surprise that conformational changes from open to closed form of individual molecules when sandwiched between graphene point contacts lead to the conductance switching of devices from the off state to the on state, consistent with the experimental observation above.

In addition to the switching effect, we also found that the on/off ratios are very high, gradually increasing from 60 for **1** and 200 for **2** to 300 for **3**. This is reasonable because among these three molecules, the transmission spectrum of the closed form for **3** shows the largest difference in comparison with that for the open form (Figure 2, Figure S6, and Table S3). This is in excellent agreement with our original design (Figure 1), which implies that the on/off conductance ratios highly depend on the side groups outside the switching core for single-molecule junctions.[4] Thus, the conductance switching is dominated by the changes in the molecular energy levels as a result of either conformation transformation or the side group substitution. These optoelectronic switching phenomena are very reproducible since we observed the consistent photoswitching effect in many devices (at least 19 working devices for **1**, 7 for **2,** and 13 for **3**).

Both afore-achieved theoretical and experimental results demonstrate that photoisomerization of diarylethenes between open/closed states is able to change the molecular energy levels at the contact interface, thus offering a chance to study intrinsic charge-transport mechanisms in molecular junctions. In most instances, charge transport in molecular junctions can be simplified as electron tunneling through a barrier (Figure 3 a).[11] In the zero-bias limit, the shape of the

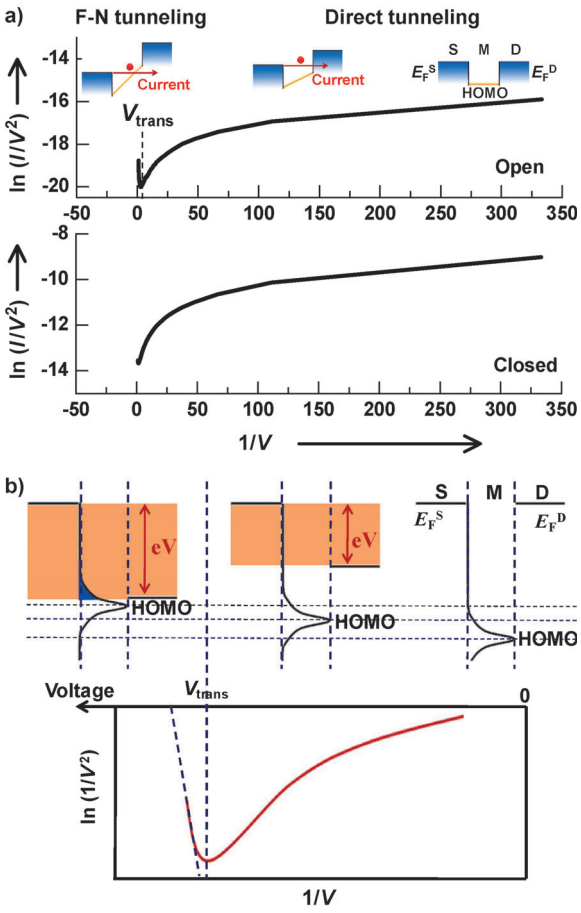

Figure 3. a) F-N plots of the *I–V* characteristics for the same **2**-reconnected molecular junction used in Figure 2 with open (top) and closed (bottom) states. The insets show the conventional barrier model to qualitatively explain the inflection of the F-N curve. E_F^S and E_F^D are the Fermi energies of source and drain electrodes, and V_{trans} is the voltage at which the inflection takes place. Note that the figures are drawn for HOMO-mediated electron tunneling. b) The resonant tunneling model to qualitatively explain the inflection of the F-N curves.

tunneling barrier is rectangular. When the applied bias exceeds the barrier height, the shape of the barrier changes to be triangular, and the Fowler–Nordheim (F-N) tunneling or field emission occurs (Figure 3 a insets). From the plot of $\ln(I/V^2)$ against V^{-1} (F-N plot), an inflection point (V_{trans}) can be obtained, which is equal to the effective barrier height and corresponds to the energy offset between the Fermi level of the electrode and the closest frontier molecular orbital. Figure 3 a shows the typical F-N plots of the *I–V* characteristics with open/closed states for the same **2**-bridged molec-

ular junction used in Figure 2a (More data for **1** and **3** can be found in Figure S9). We found that V_{trans} of the open state of **2** was about 0.41 V, less than that of the closed state (about 0.69 V). Similar data were also obtained in **1** (about 0.73 and 0.96 V for the open/closed states, respectively). Interestingly, in the case of **3**, we achieved V_{trans} of about 0.63 V for the open state, but a smaller V_{trans} value of about 0.28 V for the closed state, which is opposite to the findings in **1** and **2**. This observation should be ascribed to changes in the electronic structures of the molecule–electrode contacts as shown in Figure 1c, again proving the capability of modulating the molecular energy levels at the contact interface by molecular design (and thus the molecule–electrode coupling). For **3**-reconnected molecular junctions in which the work function of graphene locates well between HOMO and LUMO in both conformations, the charge-transport mechanism perfectly fits to the barrier model shown in Figure 3a. The effective barrier height for charge transport in the closed state is lower than that of the open state. This is in excellent consistence with the theoretical calculations which shows that the HOMO level dominating charge transport is closer to the work function of graphene for the closed form in comparison with the case of the open form (Figure 1c and Table S2). Importantly, this is direct evidence for experimentally observing the photogated V_{trans} transition when the charge-transport mechanism varies from a direct to the Fowler–Nordheim (F-N) tunneling.

In addition to the simple tunneling barrier model, another more real model for electron transport is the resonant tunneling, which can clearly explain the V_{trans} transition observed above even for **1** and **2** in which the work function of graphene is lower than the HOMO energy level of the closed form of molecules (Figure 1c). On the basis of the Landauer formula[12] and theoretical predictions,[13] the inflection in the F-N plot takes place when a certain amount of the tail of the resonant peak enters the bias window (Figure 3b). Therefore, to better reveal the transition mechanism, we systematically calculated the transmission spectra under the different biases from 0 to 1.0 V, in which we have taken into the account the polarization effects arising from the electric field (Figure 4 and Figures S10–S13).[14] Using a **2**-reconnected molecular junction as a representative, we found that when the bias reached 0.5 V in the open state, the transmission peak of the HOMO began to come into the bias window, thus providing an additional conductive channel (Figure 4a). Furthermore, from the MPSH spectra (Figure S11a), the slight increase of the HOMO delocalization was also observed at the bias of 0.5 V. These should contribute to the inflection in the F-N plot as the resonant tunneling occurs. As for the closed state of **2**, the transmission peaks are much closer to the electrode Fermi level because of the decreased HOMO–LOMO gap and thus the transmission peak of the HOMO comes into the bias window at a smaller bias (0.2 V). However, the strength of the transmission peak is very low (about 10^{-4}), which has the negligible contribution to the conductance. But, when the bias increased to 0.7 V, we observed an obvious increase of the transmission peak strength probably because of the polarization effect under the enhanced electric field (Figure 4b). On the other hand, we also detected a significant decrease of the LUMO delocalization in the MPSH spectra at the same bias (Figure S11b). This might be due to the quantum interference or other quantum effects[15] by which the decreased LUMO state leads to the higher transmission peak of the HOMO. Therefore, it is because of the enhanced transmission peak strength that the inflection of the F-N plot emerges at a bias of 0.7 V for the closed state of **2**. The same analysis for a **1**-reconnected junction generates very similar results: $V_{trans} = 0.7$ and > 1.0 V for open and closed states, respectively (Figure S12). In the case of **3**, however, the opposite values were achieved, 0.6 V for the open state and 0.1 V for the closed state (Figure S13). These results are consistent with the experimental observations as well as the discussions using the barrier model.

In summary, this study demonstrates the ability to integrate electronic functions based on molecules into electronic nanocircuits. We achieved optoelectronic switching from the off state to the on state when individual photochromic diarylethenes sandwiched between graphene point contacts transform between two states of conjugation. Spectroscopic analyses based on both barrier and resonant tunneling models prove the tunability of the molecule–electrode coupling strength through molecular engineering and consistenty support the experimental observation of the photogated tunneling transition in molecular junctions. This demonstration also provides novel insight into designing new types of molecule-based devices for revealing the relationship between charge-transport mechanisms and the electronic structures of molecular junctions.

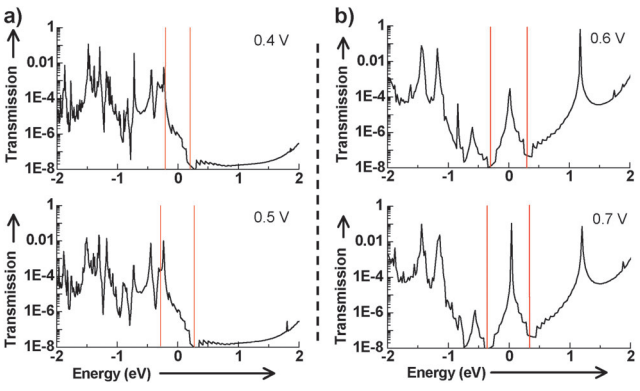

Figure 4. Transmission spectra of **2**-reconnected molecular junctions with the a) open and b) closed conformations at different biases.

Received: May 19, 2013
Published online: July 1, 2013

Keywords: charge transfer · diarylethene compounds · graphene · molecular devices · optoelectronics

[1] a) A. Aviram, M. A. Ratner, *Chem. Phys. Lett.* **1974**, *29*, 277–283; b) M. Galperin, M. A. Ratner, A. Nitzan, A. Troisi, *Science* **2008**, *319*, 1056–1060; c) R. L. McCreery, A. J. Bergren, *Adv. Mater.* **2009**, *21*, 4303–4322.

[2] a) N. Weibel, S. Grunder, M. Mayor, *Org. Biomol. Chem.* **2007**, *5*, 2343–2353; b) C. Jia, X. Guo, *Chem. Soc. Rev.* **2013**, *42*, 5642–5660; c) A. K. Feldman, M. L. Steigerwald, X. Guo, C. Nuckolls,

Acc. Chem. Res. **2008**, *41*, 1731 – 1741; d) H. Song, M. A. Reed, T. Lee, *Adv. Mater.* **2011**, *23*, 1583 – 1608.
[3] a) M. Irie, *Chem. Rev.* **2000**, *100*, 1685 – 1716; b) B. L. Feringa, *Acc. Chem. Res.* **2001**, *34*, 504 – 513.
[4] a) J. Li, G. Speyer, O. F. Sankey, *Phys. Rev. Lett.* **2004**, *93*, 248302; b) J. Huang, Q. X. Li, H. B. Su, J. L. Yang, *Chem. Phys. Lett.* **2009**, *479*, 120 – 124; c) M. K. Ashraf, N. A. Bruque, J. L. Tan, G. J. O. Beran, R. K. Lake, *J. Chem. Phys.* **2011**, *134*, 024524.
[5] a) J. He, F. Chen, P. A. Liddell, J. Andreasson, S. D. Straight, D. Gust, T. A. Moore, A. L. Moore, J. Li, O. F. Sankey, S. M. Lindsay, *Nanotechnology* **2005**, *16*, 695 – 702; b) N. Katsonis, T. Kudernac, M. Walko, S. J. van der Molen, B. J. van Wees, B. L. Feringa, *Adv. Mater.* **2006**, *18*, 1397 – 1400; c) S. J. van der Molen, J. H. Liao, T. Kudernac, J. S. Agustsson, L. Bernard, M. Calame, B. J. van Wees, B. L. Feringa, C. Schonenberger, *Nano Lett.* **2009**, *9*, 76 – 80; d) Y. Kim, T. J. Hellmuth, D. Sysoiev, F. Pauly, T. Pietsch, J. Wolf, A. Erbe, T. Huhn, U. Groth, U. E. Steiner, E. Scheer, *Nano Lett.* **2012**, *12*, 3736 – 3742; e) D. Dulic, S. J. van der Molen, T. Kudernac, H. T. Jonkman, J. J. D. de Jong, T. N. Bowden, J. van Esch, B. L. Feringa, B. J. van Wees, *Phys. Rev. Lett.* **2003**, *91*, 207402; f) A. C. Whalley, M. L. Steigerwald, X. Guo, C. Nuckolls, *J. Am. Chem. Soc.* **2007**, *129*, 12590 – 12591.
[6] T. Tsujioka, M. Irie, *J. Photochem. Photobiol. C* **2010**, *11*, 1 – 14.
[7] a) K. Moth-Poulsen, T. Bjornholm, *Nat. Nanotechnol.* **2009**, *4*, 551 – 556; b) S. Liu, Z. Wei, Y. Cao, L. Gan, Z. Wang, W. Xu, X. Guo, D. Zhu, *Chem. Sci.* **2011**, *4*, 796 – 802.
[8] W. R. Browne, J. J. D. de Jong, T. Kudernac, M. Walko, L. N. Lucas, K. Uchida, J. H. van Esch, B. L. Feringa, *Chem. Eur. J.* **2005**, *11*, 6414 – 6429.
[9] a) Y. Cao, S. H. Dong, S. Liu, L. He, L. Gan, X. M. Yu, M. L. Steigerwald, X. S. Wu, Z. F. Liu, X. Guo, *Angew. Chem.* **2012**, *124*, 12394 – 12398; *Angew. Chem. Int. Ed.* **2012**, *51*, 12228 – 12232; b) Y. Cao, S. H. Dong, S. Liu, Z. F. Liu, X. Guo, *Angew. Chem.* **2013**, *125*, 3998 – 4002; *Angew. Chem. Int. Ed.* **2013**, *52*, 3906 – 3910.
[10] C. Jia, J. Jiang, L. Gan, X. Guo, *Sci. Rep.* **2012**, *2*, 707.
[11] J. M. Beebe, B. Kim, J. W. Gadzuk, C. D. Frisbie, J. G. Kushmerick, *Phys. Rev. Lett.* **2006**, *97*, 026801.
[12] Y. Imry, R. Landauer, *Rev. Mod. Phys.* **1999**, *71*, S306 – S312.
[13] M. Araidai, M. Tsukada, *Phys. Rev. B* **2010**, *81*, 235114.
[14] J. Taylor, H. Guo, J. Wang, *Phys. Rev. B* **2001**, *63*, 245407.
[15] C. M. Guédon, H. Valkenier, T. Markussen, K. S. Thygesen, J. C. Hummelen, S. J. van der Molen, *Nat. Nanotechnol.* **2012**, *7*, 305 – 309.